



## Aerodynamic Analysis of Trailing Edge Enlarged Wind Turbine Airfoils

Xu, Haoran; Shen, Wen Zhong; Zhu, Wei Jun; Yang, Hua; Liu, Chao

*Published in:*  
Journal of Physics: Conference Series (Online)

*Link to article, DOI:*  
[10.1088/1742-6596/524/1/012010](https://doi.org/10.1088/1742-6596/524/1/012010)

*Publication date:*  
2014

*Document Version*  
Publisher's PDF, also known as Version of record

[Link back to DTU Orbit](#)

*Citation (APA):*  
Xu, H., Shen, W. Z., Zhu, W. J., Yang, H., & Liu, C. (2014). Aerodynamic Analysis of Trailing Edge Enlarged Wind Turbine Airfoils. *Journal of Physics: Conference Series (Online)*, 524(1), Article 012010. <https://doi.org/10.1088/1742-6596/524/1/012010>

---

### General rights

Copyright and moral rights for the publications made accessible in the public portal are retained by the authors and/or other copyright owners and it is a condition of accessing publications that users recognise and abide by the legal requirements associated with these rights.

- Users may download and print one copy of any publication from the public portal for the purpose of private study or research.
- You may not further distribute the material or use it for any profit-making activity or commercial gain
- You may freely distribute the URL identifying the publication in the public portal

If you believe that this document breaches copyright please contact us providing details, and we will remove access to the work immediately and investigate your claim.

## Aerodynamic Analysis of Trailing Edge Enlarged Wind Turbine Airfoils

This content has been downloaded from IOPscience. Please scroll down to see the full text.

2014 J. Phys.: Conf. Ser. 524 012010

(<http://iopscience.iop.org/1742-6596/524/1/012010>)

View [the table of contents for this issue](#), or go to the [journal homepage](#) for more

Download details:

IP Address: 192.38.90.17

This content was downloaded on 20/06/2014 at 09:26

Please note that [terms and conditions apply](#).

# Aerodynamic Analysis of Trailing Edge Enlarged Wind Turbine Airfoils

Haoran Xu<sup>1</sup>, Wenzhong Shen<sup>2</sup>, Weijun Zhu<sup>2</sup>, Hua Yang<sup>1</sup> and Chao Liu<sup>1</sup>

<sup>1</sup> College of Water Resources and Energy Power Engineering, Yangzhou University, Yangzhou 225009, China

<sup>2</sup> Department of Wind Energy, Technical University of Denmark, Lyngby 2800, Denmark

E-mail: wzsh@dtu.dk

**Abstract.** The aerodynamic performance of blunt trailing edge airfoils generated from the DU-91-W2-250, DU-97-W-300 and DU-96-W-350 airfoils by enlarging the thickness of trailing edge symmetrically from the location of maximum thickness to chord to the trailing edge were analyzed by using CFD and RFOIL methods at a chord Reynolds number of  $3 \times 10^6$ . The goal of this study is to analyze the aerodynamic performance of blunt trailing edge airfoils with different thicknesses of trailing edge and maximum thicknesses to chord. The steady results calculated by the fully turbulent  $k-\omega$  SST, transitional  $k-\omega$  SST model and RFOIL all show that with the increase of thickness of trailing edge, the linear region of lift is extended and the maximum lift also increases, the increase rate and amount of lift become limited gradually at low angles of attack, while the drag increases dramatically. For thicker airfoils with larger maximum thickness to chord length, the increment of lift is larger than that of relatively thinner airfoils when the thickness of blunt trailing edge is increased from 5% to 10% chord length. But too large lift can cause abrupt stall which is profitless for power output. The transient characteristics of blunt trailing edge airfoils are caused by blunt body vortices at low angles of attack, and by the combined effect of separation and blunt body vortices at large angles of attack. With the increase of thickness of blunt trailing edge, the vibration amplitudes of lift and drag curves increase. The transient calculations over-predict the lift at large angles of attack and drag at all angles of attack than the steady calculations which is likely to be caused by the artificial restriction of the flow in two dimensions.

## Nomenclature

$R$	radius of the rotor
$\alpha$	angle of attack
$C_l, C_d$	lift and drag coefficients
$C_{lmax}$	maximum value of $C_l$
$t$	time
$t_{th}$	maximum thickness of airfoil
$c$	chord length of airfoil
$t_{te}$	thickness of trailing edge
SPL	sound pressure level



RANS Reynolds-Averaged Navier-Stokes  
DES Detached Eddy Simulation  
LES Large Eddy Simulation

## 1. Introduction

With the increase of wind turbine's size, the design of inboard parts of wind turbine blades involves more factors such as aerodynamic performance, manufacturing costs, structure demands, compatibility and so on. For aerodynamic performance, though the inboard part of large wind turbine blades contributes less to the overall torque generated by the entire blade than the outboard part due to relatively small arm of force, the improvement of aerodynamic performance for the inboard part can still increase the total power output of wind turbines. For structure demands, the inboard parts of the blade bear larger bending moment, so the structure characteristics of airfoils used in this part should be strong enough to bear the load. In view of this, flat back or blunt trailing edge airfoils which can meet the aforementioned requirements have been presented to be used as the airfoils in the region from  $20\%R$  to  $40\%R$ <sup>[1]</sup> of large scale wind turbine blades<sup>[1,2,3]</sup>. From the structural view, blunt trailing edge airfoils have larger sectional area than that of sharp trailing edge airfoils with the same maximum thickness  $t_{th}$  and chord length  $c$ , thus the sectional moment inertia is increased, the bending and distorting capacity are strengthened. On the aerodynamic performance, blunt trailing edge airfoils have a higher lift curve slope, a higher maximum lift and a lower sensitivity to surface contamination<sup>[2]</sup>.

Previous work about analyzing the performance of airfoils with blunt trailing edge includes wind tunnel experiment at given Reynolds numbers<sup>[4,5,6,7]</sup>, CFD method for blunt trailing edge airfoils<sup>[8,9]</sup> as well as the effect on rotor performance<sup>[10]</sup>. While, these advantages of blunt trailing edge airfoils are obtained at the cost of increased aerodynamic noise and aerodynamic drag<sup>[4]</sup>. Mathew et al<sup>[4]</sup> presented that a splitter plate attached to the blunt edge can reduce the overall SPL of a blunt trailing edge airfoil. Baker et al<sup>[5]</sup> showed that double splitter plate configuration and serrations on the downstream edge of the splitter plates can cause a drag reduction and improve the performance compared to a non-serrated blunt edge.

The main purpose of this research is to analyze the steady aerodynamic performance of blunt trailing edge airfoils with different  $t_{te}$  for wind turbines by using CFD method and RFOIL<sup>[11]</sup> which is a modified version of XFOIL<sup>[12]</sup>, analyze the transient performance especially the vortex shedding and vibration characteristics of lift and drag curves of blunt trailing edge airfoils.

The paper is organized as follows. The airfoils, method for enlarging the trailing edge of airfoils, CFD problem setup and solution method are described in section 2. In order to validate the prediction accuracy, the validation cases are presented in section 3. The steady and unsteady aerodynamic performance of blunt trailing edge airfoils is analyzed in section 4 and section 5 respectively. Conclusion is given in section 6.

## 2. Research objective and methodology

### 2.1. Airfoils

DU series airfoils which have a  $t_{th}/c$  value ranging from 15% to 40% are designed by Delft University of Technology and widely used in wind turbine design. Blunt trailing edge airfoils are usually generated from thick airfoils ( $t_{th}/c \geq 25\%$ ). So the DU-91-W2-250, DU-97-W-300 and DU-96-W-350 airfoils whose  $t_{th}/c$  equals to 25%, 30% and 35% respectively were used as the reference airfoils in this paper.

### 2.2. Method of enlarging the trailing edge of airfoils

The geometry of a blunt trailing edge airfoil is generated by several methods. The first one is to cut off a certain part from the rear region of an existing airfoil<sup>[7]</sup>. The disadvantage of this method is that by truncating the chord, the maximum thickness to chord ratio  $t_{th}/c$  and the camber line changes, which makes it difficult to compare the aerodynamic performance of truncated airfoil with the original one. Moreover, some lift can be lost by cutting off the trailing edge. So the first method is seldom used in

recent studies. In order to isolate the influence of the blunt trailing edge, the second method called mixed function of index is used. By this method, a blunt trailing edge airfoil can be generated by symmetrically adding thickness to both sides of the middle line over some aft part of the airfoil.

In order to analyze the aerodynamic performance of blunt trailing edge airfoils with different values of  $t_{te}$ . The aforementioned method called mixed function of index was used to enlarge the thickness of trailing edge symmetrically from the location of maximum thickness to the trailing edge. In order to get smooth geometry the enlarged thickness should change in power function. The mixed function of index can be expressed as

$$\begin{cases} x = x_0, y = y_0 & (0 \leq x \leq x_t) \\ x = x_0, y = y_0 \pm 0.5\delta \left( \frac{x - x_t}{c - x_t} \right)^n & (x_t < x \leq c) \end{cases} \quad (1)$$

Where  $(x_0, y_0)$  are the coordinates of the original airfoil and  $(x, y)$  are the coordinates of the blunt trailing edge airfoil.  $\delta$  is the increased thickness of trailing edge.  $x_t$  is the x-coordinate of the location of maximum thickness. The sign  $\pm$  means increasing the thickness on both suction and pressure side of the airfoil.  $n$  is the power exponent which is used to control the smoothness of the geometry. In [13]  $n = 1.8 \sim 2.5$  suggested, and so  $n = 2$  is used in this paper.

By using this method called mixed function of index, the values of  $t_{te}$  of the three DU airfoils mentioned in subsection 2.1 are increased to  $5\%c$  and  $10\%c$ , respectively. Suffix was added to the original name of the airfoil to name the new blunt trailing edge airfoils. For example, the new name DU-97-W-300-05 means that the new blunt trailing edge airfoil is generated from DU-97-W-300 airfoil by enlarging the thickness of trailing edge to  $5\%c$ . DU-97-W-300-10 means that  $t_{te}$  of the new blunt trailing edge airfoil is  $10\%c$ .

### 2.3. CFD problem set up and solution method

The commercial Computational Fluid Dynamics software Fluent was used to predict the two dimensional aerodynamic performance of the reference and blunt trailing edge airfoils. All the calculations in this paper were performed at a chord Reynolds number of  $3 \times 10^6$ . The chord length of all airfoils is one meter in this paper. So the free stream velocity is 43.822 m/s. Predictions were performed using both two-equations Menter  $k-\omega$  SST turbulence model<sup>[14]</sup> and four-equations transitional  $k-\omega$  SST model which is a combination of the  $\gamma - \bar{R}\bar{e}_\theta$  transition model<sup>[15,16]</sup> and the  $k-\omega$  SST turbulence model.

The O-mesh topology was employed to generate the computational grids in ICEM. For the original and modified blunt trailing edge airfoils, there were 580 grid points on the airfoil surface and with clustering near the leading and trailing edges, and 100 grid points across the trailing edge base. 200 grid points were used in the radial direction of the circular calculation domain with a wall-norm grid spacing of  $5 \times 10^{-6}$  m from the airfoil surface and a stretching ratio of 1.05 to ensure that the maximum value of  $y^+$  for the first grid cell off the airfoil surface is less than 1 for both turbulence models. For transient calculations, in order to capture the phenomenon of vortex shedding from the blunt trailing edge, 300 grid points were used in the radial direction.

The calculation domain is a circular domain with a radius of  $50c$ . The airfoil surface was set as adiabatic no-slip wall boundary condition. A velocity-inlet boundary condition was applied at the inflow boundary and the pressure-outlet boundary condition was applied at the outflow boundary. The turbulence intensity of free-stream is 0.2%.

For transient calculations, in order to capture the course of vortex shedding the time step was set to 0.0001s.

### 3. Validation cases

In order to validate the computational methodologies for thick and blunt trailing edge airfoils, the aerodynamic performance of DU-97-W-300 and DU-97-W-300-10 airfoils were predicted and analyzed.

Experimental data for a DU-97-W-300 airfoil is available in literature [17], and the experimental data of DU-97-W-300-10 airfoil only at three angles of attack was presented in literature [4].

Calculations were performed using CFD and RFOIL methods. For CFD method, steady calculations were used to predict the aerodynamic performance of the DU-97-W-300 airfoil, while both steady and transient calculations were performed for the DU-97-W-300-10 airfoil. All the experimental data presented here are for clean airfoil surface.

The results calculated by the fully turbulent  $k-\omega$  SST model, transitional  $k-\omega$  SST model and RFOIL for the DU-97-W-300 airfoil are compared with experimental data in Figure 1. In terms of lift coefficient (Figure 1(a)), the data calculated by the transitional  $k-\omega$  SST model is in good agreement with experimental data when  $\alpha \leq 9$  degree, but the maximum lift is over-predicted. The results calculated by the fully turbulent  $k-\omega$  SST model are lower than the experimental data in the linear region but higher in the stall region, the reason of the underprediction in the linear region for lift is that the SST model is a fully turbulent model where transition occurs at the leading edge while the experimental data is performed for clean airfoil surface which has a free transition phenomenon on the surface. So the data calculated by the transitional  $k-\omega$  SST model agrees well with the experimental data. The results of lift is over-predicted a little by RFOIL, while in the stall region RFOIL can give better prediction especially for the prediction of stall angle than the CFD method. In terms of drag (Figure 1(b)), the results calculated by the transitional  $k-\omega$  SST model and RFOIL agree very well with experimental data in the linear part. It's well documented that RANS solvers have inadequate capability in their prediction of flow near or at stall<sup>[18]</sup>.

For the DU-97-W-300-10 airfoil which has a  $t_{ic}$  of 10% $c$ , the results calculated by both steady and transient versions and RFOIL are presented in Figure 2. For lift coefficient, the transient results are closer to the experimental data and larger than the steady ones, but the difference is small. In addition, the difference between the steady results in the linear region calculated by the fully turbulent  $k-\omega$  SST and the transitional  $k-\omega$  SST models is not as large as that presented in Figure 1(b), this indicates that the sensitivity to surface contamination of blunt trailing edge airfoils is lower than that of airfoils with a relatively sharp trailing edge. The results calculated by RFOIL are larger than the experimental data. For drag coefficients, all the computational results are inconsistent with experimental data, the steady results seems to be closer to the experimental data, while the transient results calculated by the SST model are twice of the experimental data. The flow unsteadiness may be used to explain the overprediction of transient results in Figure 2(b). For blunt trailing edge airfoils, the majority of the drag comes from the blunt trailing edge. The strength of vortices near the blunt trailing edge may be over-predicted due to the restriction of the CFD codes in two dimensions, because the blunt body wake seems to be highly three dimensional.

Generally speaking, for conventional airfoils with relatively sharp trailing edges, the transitional  $k-\omega$  SST model can give accurate prediction in the linear region for both lift and drag coefficients when the airfoil surface is clean. For blunt trailing edge airfoils, both steady and transient results calculated by SST and transition SST are in good agreement with experimental data for lift coefficients at relevant angles of attack. The transient method over-predicts the drag coefficients a lot due to the restriction of the two dimensional flows. Although the RANS solver with conventional turbulence models is ill-equipped for the prediction of stall, it's easy to find that the stall is just delayed and the general trend is reliable.

So, in the following section, the transitional  $k-\omega$  SST model is used to calculate the aerodynamic performance of blunt trailing edge airfoils with clean surface, and the fully turbulent  $k-\omega$  SST model is used to calculate the aerodynamic performance of blunt trailing edge airfoils under the condition that transition just occurs at the leading edge. Besides, RFOIL code which has a  $e^n$  transition model<sup>[19]</sup> and can work well in stall region is also used to predict the aerodynamic performance of blunt trailing edge airfoils.

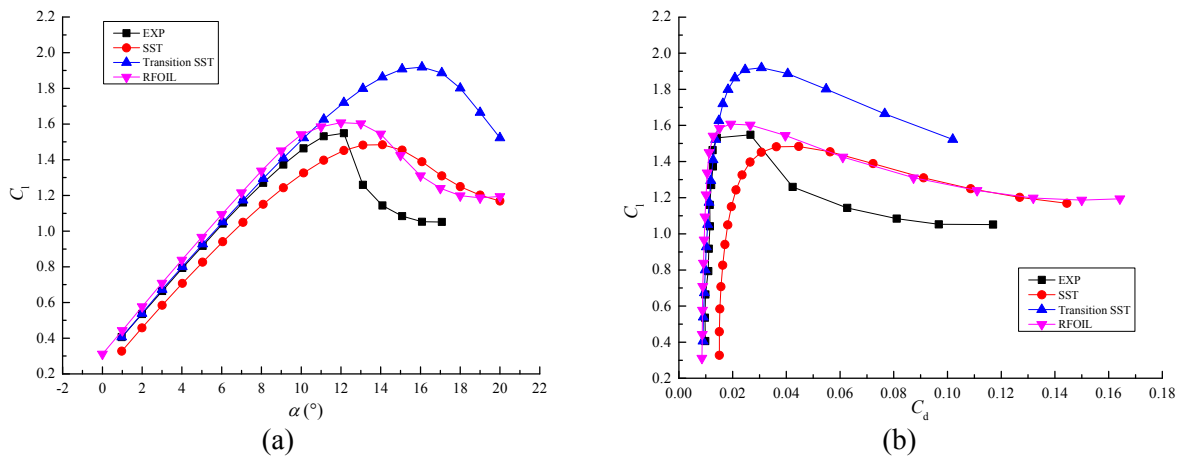


**Figure 1.** Computational and experimental (a) lift curves and (b) lift-drag polar for a DU-97-W-300 airfoil at a Reynolds number of  $3 \times 10^6$

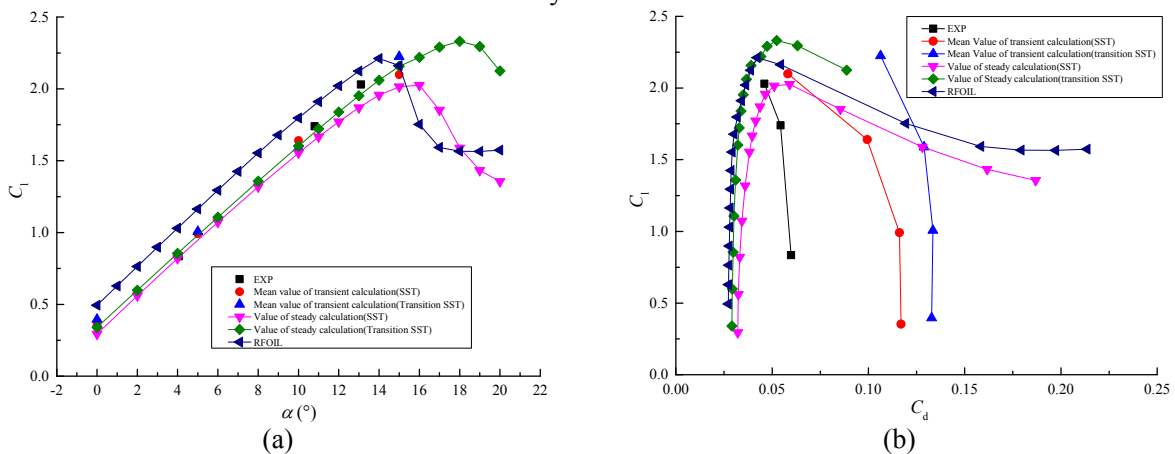


**Figure 2.** Computational and experimental (a) lift curves and (b) lift-drag polar for a DU-97-W-300-10 airfoil at a Reynolds number of  $3 \times 10^6$

#### 4. Steady aerodynamic performance of blunt trailing edge airfoils

In order to study the aerodynamic performance of blunt trailing edge airfoils with different values of  $t_{te}$  and  $t_{th}/c$ , the steady aerodynamic performance of blunt trailing edge airfoils generated from DU-91-W2-250, DU-97-W-300 and DU-96-W-350 airfoils is presented in Figure 3 to Figure 5. On one hand, from Figure 3 to Figure 5, it's easy to find that, all computational methods present similar results. Blunt trailing edge airfoils have higher lift, lift curve slope, maximum lift and larger linear region than the conventional airfoils. When  $t_{te}$  is increased from the value of original airfoil to  $5\%c$ , the increment of lift coefficients is greater than that when  $t_{te}$  is increased from  $5\%c$  to  $10\%c$  at low angles of attack. Besides, when  $t_{te}$  is increased from  $5\%c$  to  $10\%c$ , the increment of lift at small angles of attack is limited in Figure 3(b), while the drag increases rapidly. In order to find out the quantitative increment of lift for blunt trailing edge airfoils with different values of  $t_{te}$  and  $t_{th}/c$ , the lift coefficient increment of the blunt trailing edge airfoils relative to the original ones is presented in Figure 6. The results calculated by the fully turbulent  $k-\omega$  SST model are only taken to be analyzed. In Figure 6, it's clear to find that the increment of lift coefficients when  $t_{te}$  is increased from the value of the original airfoil to  $5\%c$  is larger than that when  $t_{te}$  is increased from  $5\%c$  to  $10\%c$  at low angles of attack. In addition, for thicker airfoils with larger value of  $t_{th}/c$ , the increment of lift coefficient when  $t_{te}$  is increased from  $5\%c$  to  $10\%c$  is larger than that for relatively thinner airfoils.

On the other hand, from Figure 3 to Figure 5, it's obvious to find that the lift of a blunt trailing edge airfoil with a  $t_{te}$  of  $10\%c$  drops down more quickly than that of the airfoil with a  $t_{te}$  of  $5\%c$  and the original airfoil after it reaches the maximum value for either thicker airfoils or relatively thinner airfoils. Thus, with the increase of  $t_{te}$ , the maximum lift also increases, but one problem comes up with the increase of maximum lift, too large maximum lift may cause abrupt stall which may lead to instability of power output.

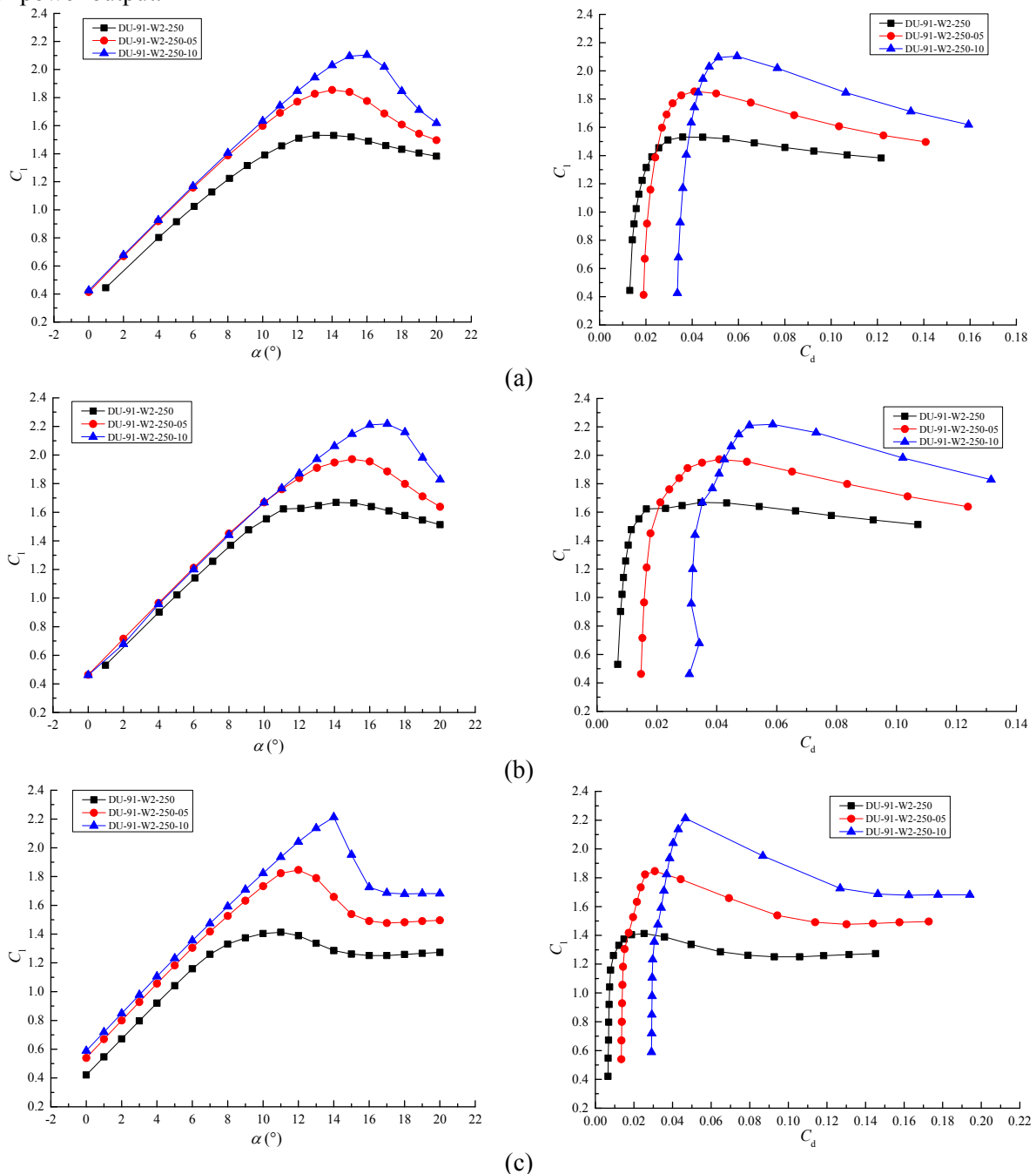


**Figure 3.** Lift curves and lift-drag polar for the DU-91-W2-250, DU-91-W2-250-05 and DU-91-W2-250-10 airfoils calculated by (a) SST, (b) transition SST and (c) RFOIL at a chord Reynolds number of  $3 \times 10^6$



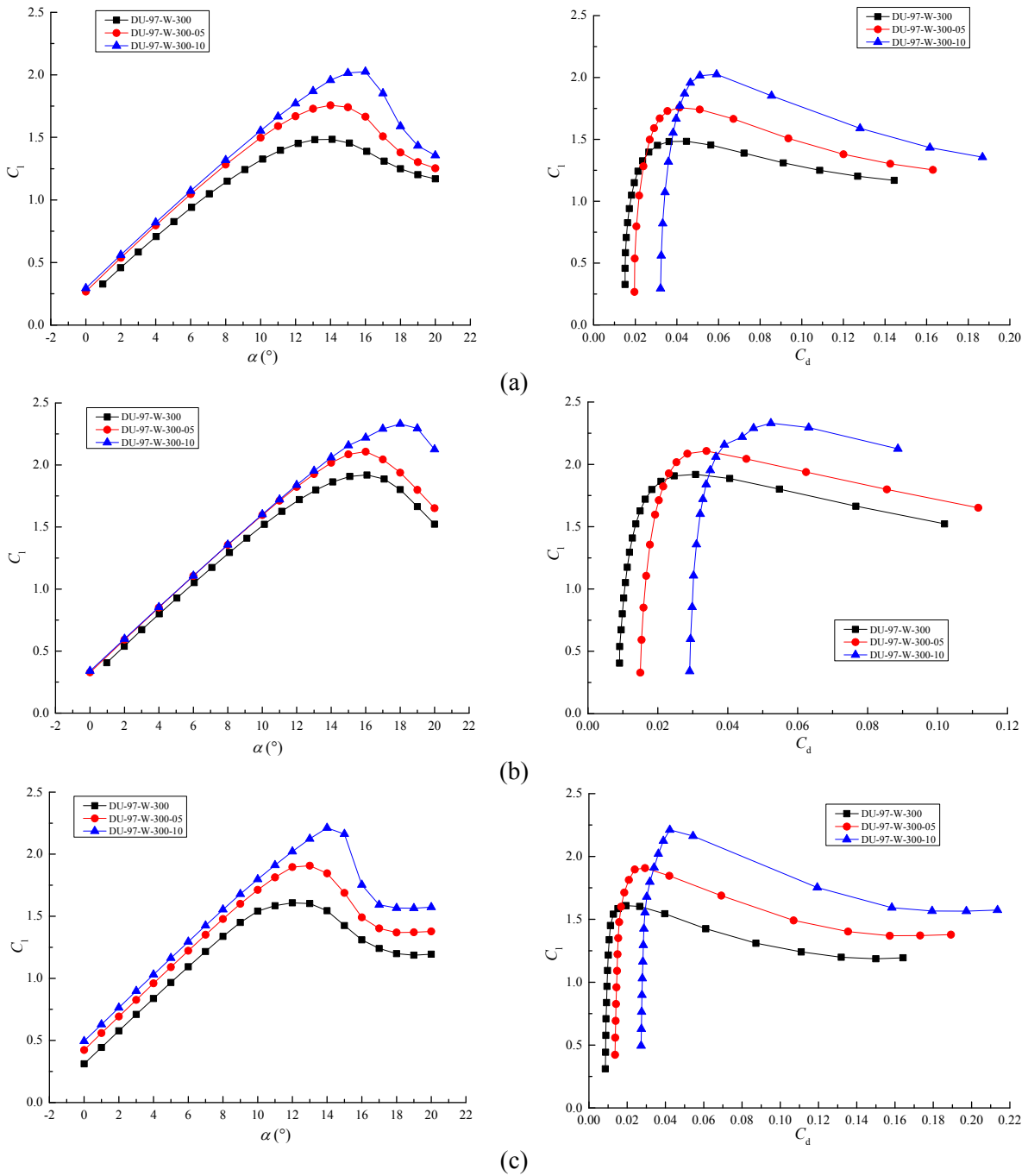


**Figure 4.** Lift curves and lift-drag polar for the DU-97-W-300, DU-97-W-300-05 and DU-97-W-300-10 airfoils calculated by (a) SST, (b) transition SST and (c) RFOIL at a chord Reynolds number of  $3 \times 10^6$

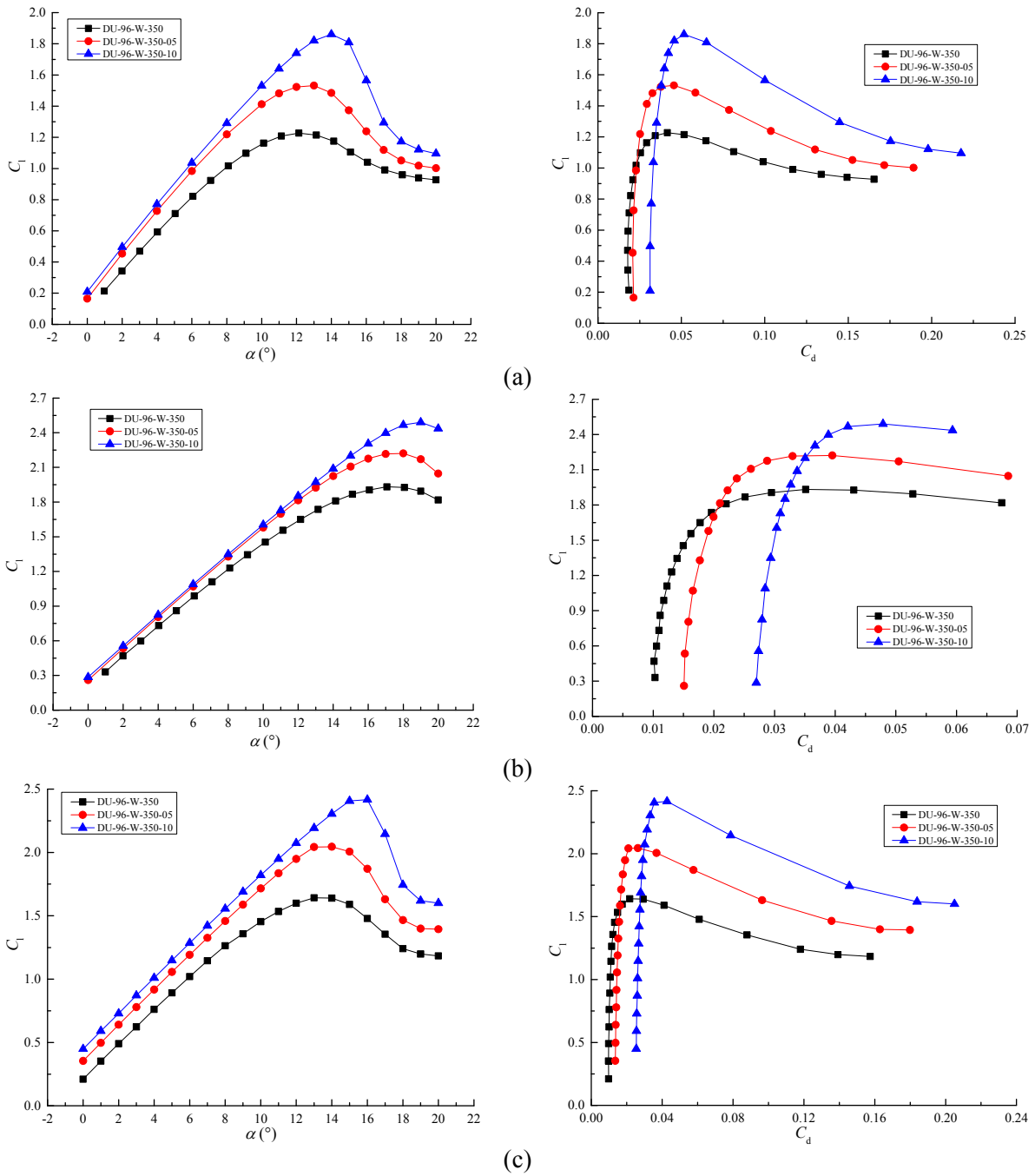


**Figure 5.** Lift curves and lift-drag polar for the DU-96-W-350, DU-96-W-350-05 and DU-96-W-350-10 airfoils calculated by (a) SST, (b) transition SST and (c) RFOIL at a chord Reynolds number of  $3 \times 10^6$

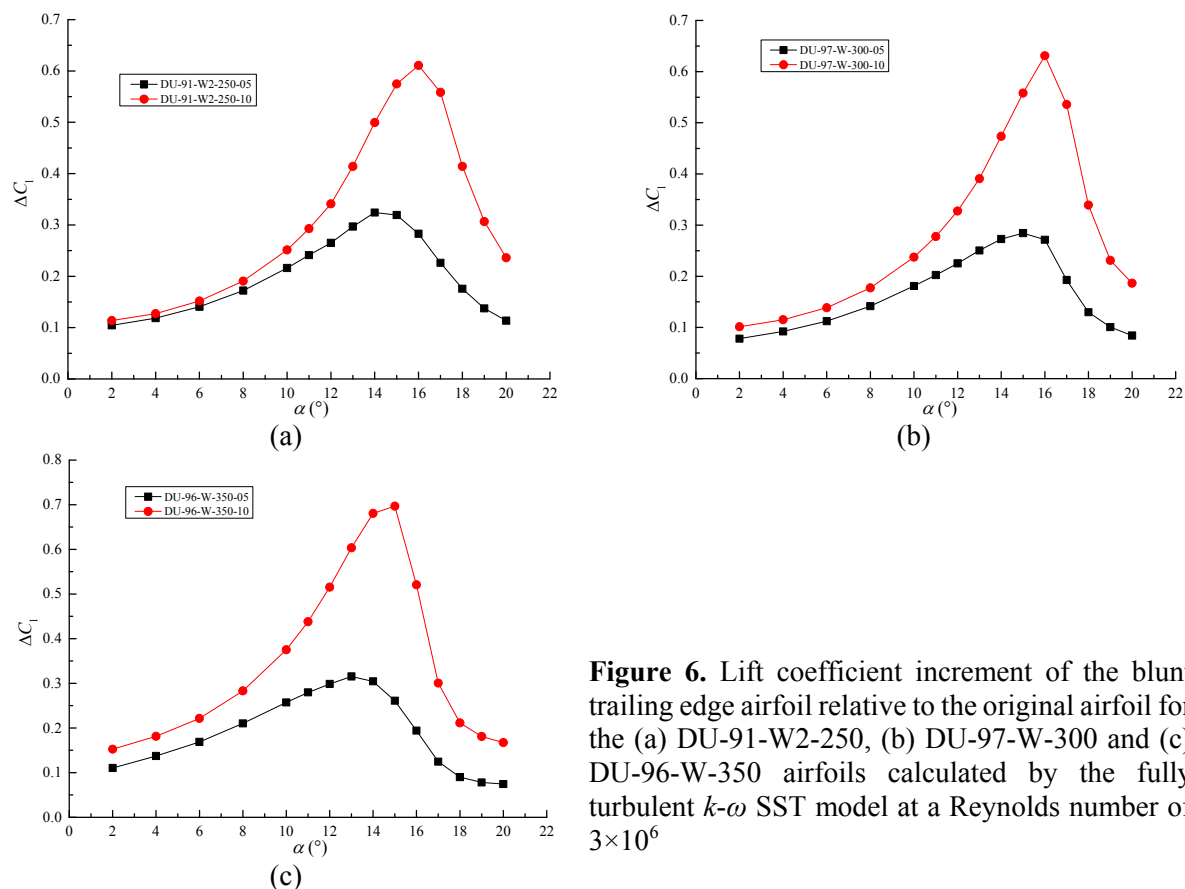


**Figure 6.** Lift coefficient increment of the blunt trailing edge airfoil relative to the original airfoil for the (a) DU-91-W2-250, (b) DU-97-W-300 and (c) DU-96-W-350 airfoils calculated by the fully turbulent  $k-\omega$  SST model at a Reynolds number of  $3 \times 10^6$

All in all, for the blunt trailing edge airfoils generated from three airfoils with different values of  $t_{th}/c$ , the increment of lift coefficient becomes limited gradually at low angles of attack when increasing  $t_{te}$ . Though with the increase of  $t_{te}$ , the linear region of lift curve is extended and the maximum lift increases to a very high level, the abrupt stall occurs due to the high maximum lift. Because the blunt trailing edge airfoils used in the inboard region of a blade often operate at large angles of attack, abrupt stall may cause the instability of power output. Besides, with the increase of  $t_{te}$ , the drag of airfoils increases dramatically. In the abrupt stall region, the lift drops down quickly while the drag increases quickly, the efficiency of the airfoil may fall down hastily. Thus, the value of  $t_{te}$  should be restrained in a certain range, finite thickness can be beneficial.

## 5. Transient aerodynamic performance of blunt trailing edge airfoils

### 5.1. Transient characteristics of lift and drag curves

In order to study the transient aerodynamic performance of blunt trailing edge airfoils, the transient calculations for the DU-97-W-300-05 and DU-97-W-300-10 airfoils were performed at  $0^\circ$ ,  $5^\circ$ ,  $10^\circ$ ,  $15^\circ$ ,  $20^\circ$ ,  $25^\circ$  angles of attack with a chord Reynolds number of  $3 \times 10^6$  by the fully turbulent  $k-\omega$  SST model.

Compared with conventional airfoils, blunt trailing edge airfoils have a larger  $t_{te}$  which can cause vortex generation and shedding, the aerodynamic performance of blunt trailing edge airfoils appears to have a periodic characteristic while the conventional airfoils only have this periodic characteristic at large angles of attack. In order to compare the transient aerodynamic performance of blunt trailing edge airfoils at different angles of attack, the lift and drag curves with five periods for  $0^\circ$ ,  $5^\circ$ ,  $10^\circ$ ,  $15^\circ$ ,  $20^\circ$ ,  $25^\circ$  angles of attack are presented in Figure 7.

For the DU-97-W-300-05 airfoil, when  $\alpha=0^\circ$  and  $\alpha=5^\circ$ , the amplitude and period of the lift curve are similar to each other. When  $\alpha=10^\circ$  and  $\alpha=15^\circ$ , the lift curve is a straight line approximately. When  $\alpha=20^\circ$

and  $\alpha=25^\circ$ , both the amplitude and period of lift curve increase with the increase of angle of attack. The vibration characteristic of drag curve is similar to the lift curve, but there are serrations in drag vibration curve when  $\alpha=25^\circ$ .  $\alpha=10^\circ$  and  $\alpha=15^\circ$  can be considered as transitive angles of attack, the lift and drag are steady or vibrate slightly under these angles of attack.

For the DU-97-W-300-10 airfoil, when  $\alpha=0^\circ$ ,  $\alpha=5^\circ$  and  $\alpha=10^\circ$ , the amplitude and period of the lift curve are similar but much larger than that of the DU-97-W-300-05 airfoil. Only when  $\alpha=15^\circ$ , the lift curve vibrates very slightly. When  $\alpha=20^\circ$  and  $\alpha=25^\circ$ , both amplitude and period of the lift curve increase with angle of attack. The vibration characteristic of the drag curve is similar to that of the lift curve, similarly, there are serrations in the drag vibration curve when  $\alpha=25^\circ$ .

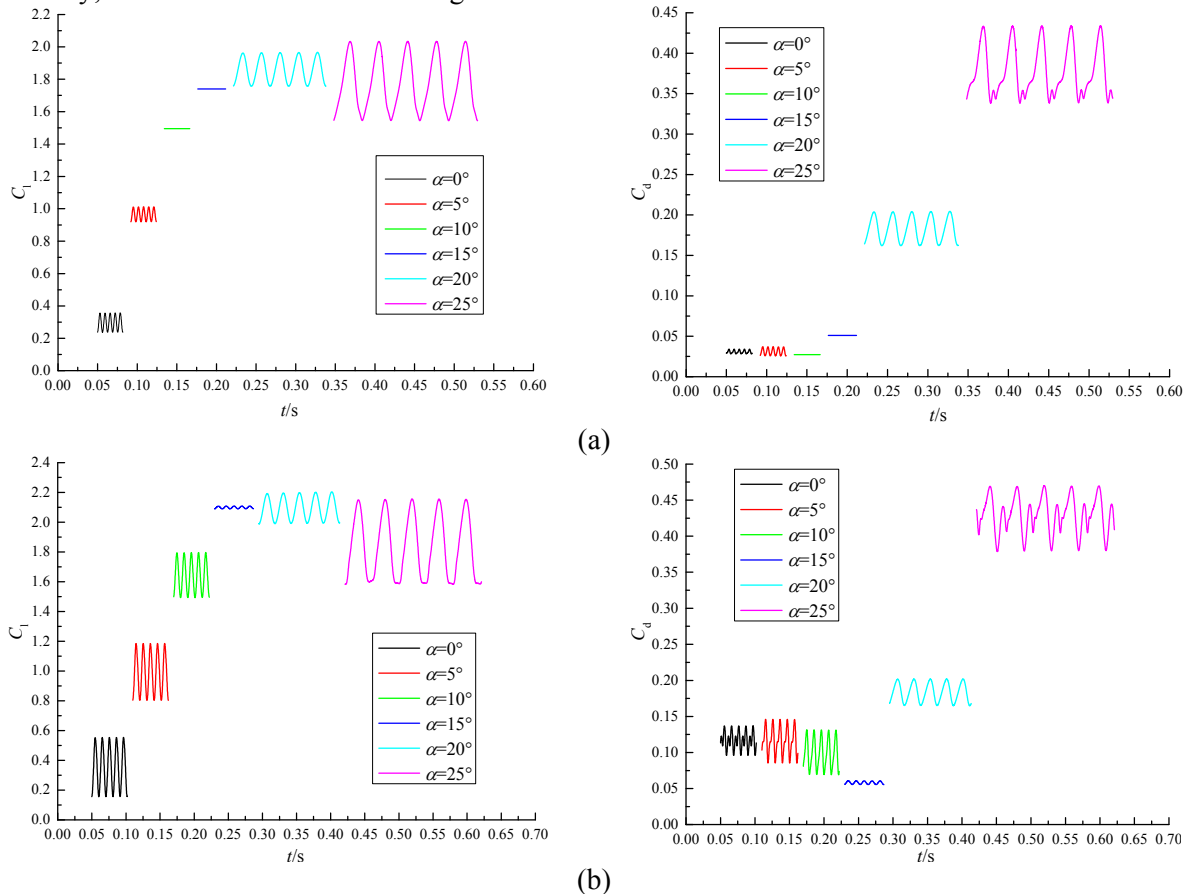


**Figure 7.** Lift and drag coefficients of the blunt trailing edge airfoils (a) DU-97-W-300-05 and (b) DU-97-W-300-10 at transient conditions

The transient aerodynamic characteristics of blunt trailing edge airfoils are mainly caused by the generation, motion and shedding of wake vortices. In order to analyze the influence of vortices on lift, the contours of vorticity at five representative moments in one period of lift curve for the DU-97-W-300-10 airfoil at different angles of attack are presented in Figure 8. When  $\alpha=0^\circ$ ,  $5^\circ$  and  $10^\circ$ , the shedding vortices are mainly blunt trailing edge vortices which shed at the upper and lower sharp corner of the blunt trailing edge. When  $\alpha=15^\circ$ , the vortices shed at a position that is relatively far away from the airfoil. When  $\alpha=20^\circ$  and  $25^\circ$ , flow separation occurs on the suction side and large separation vortices generate near the trailing edge, at the same time a backward vortex generates in the bottom part of the trailing edge. So, the size of vortex and the shedding position of vortices together influence the aerodynamic characteristics of airfoils. The larger the vortex is, the larger amplitude of the lift curve is and the longer the period of the lift curve is. The more far away from the airfoil the shedding point is, the smaller the amplitude of the lift curve is. In addition, it's easy to find that the lift curve rises to its maximum value when the upper vortex (clockwise vortex) sheds, while when the lower vortex (anticlockwise vortex)

sheds the lift curve falls down to the minimum value. The influence of shedding vortices on drag is similar to that on lift, the difference is that the generation of lower vortex is different from the generation of separation vortex on the upper side when  $\alpha=25^\circ$ , thus serrations appear in the drag curve.

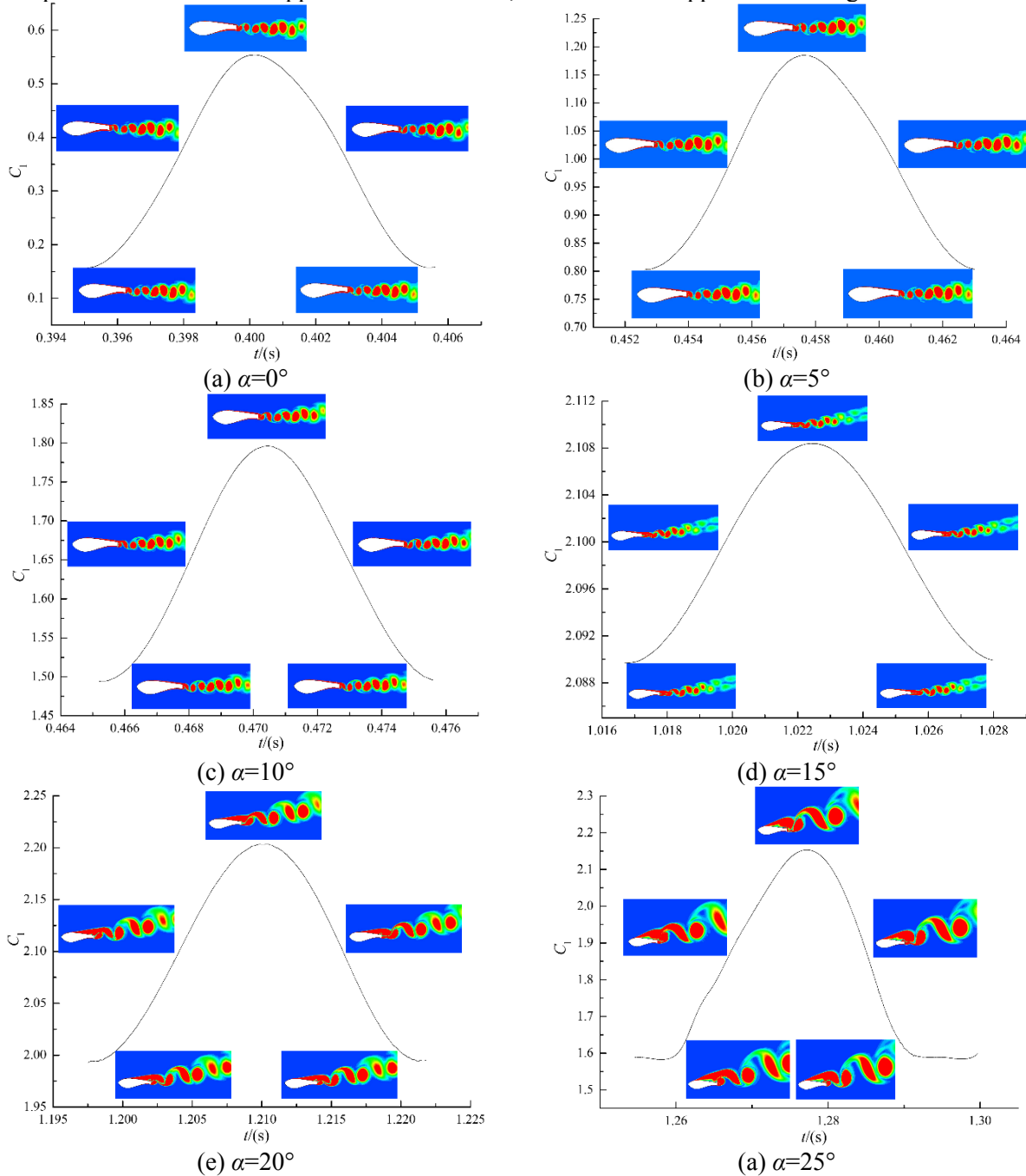


**Figure 8.** Contour of vorticity at 5 representative moments on periodic lift curves for the DU-97-W-300-10 airfoil

### 5.2. Comparison between transient and steady results

It's mentioned in section 3 that the mean value of the transient drag is much larger than the steady one and experimental data for the DU-97-W-300-10 airfoil. In order to compare the difference further, the comparison between the transient and steady results calculated by fully turbulent  $k-\omega$  SST for the DU-97-W-300-05 and DU-97-W-300-10 airfoils are presented in Figure 9.

For the DU-97-W-300-05 airfoil, the difference between the steady and transient lift curve is very small when  $\alpha \leq 15^\circ$ , but when  $\alpha = 20^\circ$  and  $25^\circ$ , the mean value of the transient lift is larger than the steady value. The mean value of the transient drag is larger than the steady value overall.

For the DU-97-W-300-10, the mean value of the transient lift is a little larger than the steady value when  $\alpha \leq 15^\circ$ , but the difference is small. When  $\alpha = 20^\circ$  and  $25^\circ$ , the mean value of the transient lift is also larger than the steady value. While the mean value of the transient drag is too much larger than the steady value when  $\alpha = 0^\circ, 5^\circ$  and  $10^\circ$ .

The vortex structure presented in Figure 8 is probably qualitatively right, but the strength of vortex is likely to be over-predicted because of the artificial restriction of the flow to be two dimensional. Transient flows such as stall for airfoil, blunt trailing edge wake seems to be highly three dimensional. This point may be used to explain the overprediction of lift at higher angles of attack and drag. Three dimensional calculations for blunt trailing edge airfoils should be performed to validate this further.

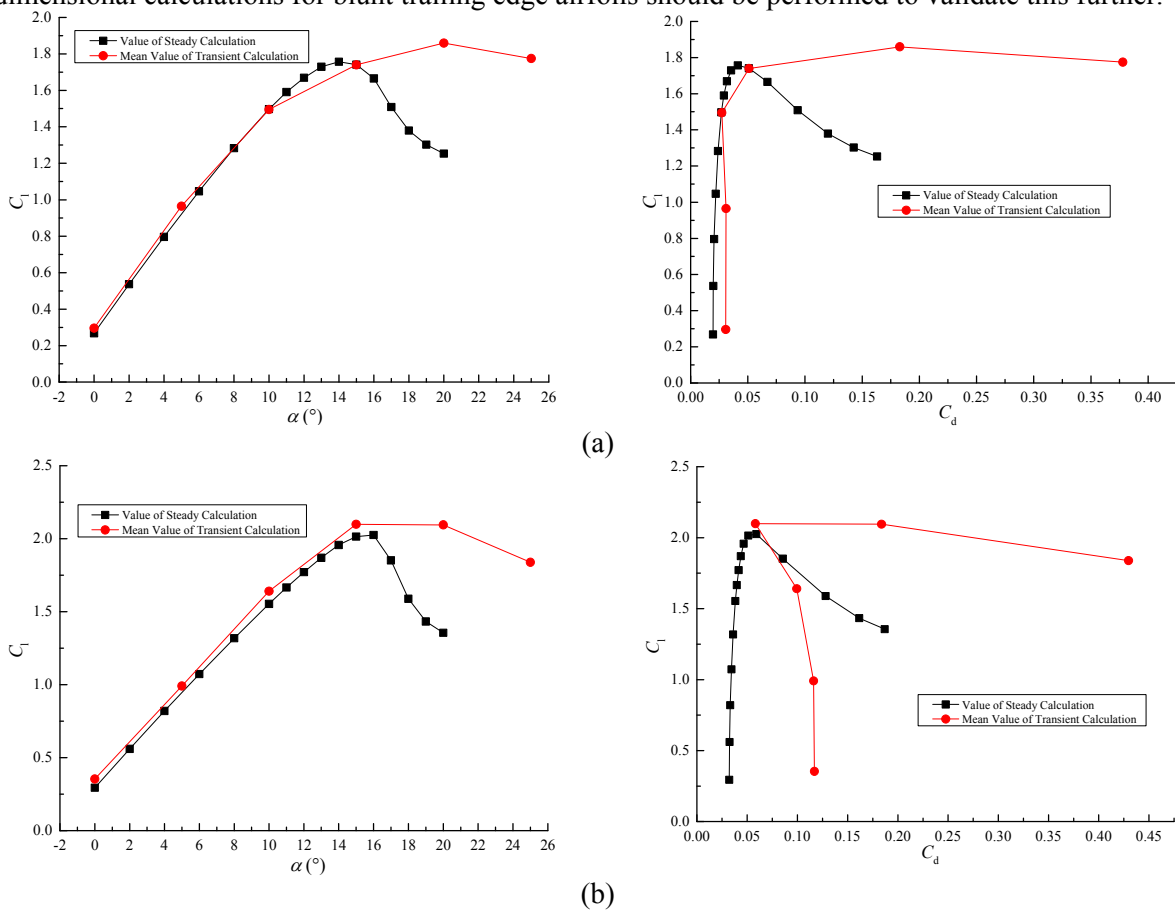


**Figure 9.** Comparison between steady and transient lift curves and lift-drag ploors of the (a) DU-97-W-300-05 and (b) DU-97-W-300-10 airfoils

**6. Conclusions**

Computational results have been presented for blunt trailing edge airfoils generated from DU-91-W2-250, DU-97-W-300 and DU-96-W-350 airfoils by enlarging the thickness of trailing edge to 5% and 10% chord length symmetrically from the location of maximum thickness to chord to the trailing edge, operating at a chord Reynolds number of  $3 \times 10^6$ . The increases of lift curve slope and maximum lift are also observed in this research. Both steady and transient calculations can predict the lift accurately in the linear region for blunt trailing edge airfoils. For drag prediction, both steady and transient calculations can't give accurate results, the transitional  $k-\omega$  SST model which is good for the prediction of drag of conventional airfoils with a relatively sharp trailing edge at low angles of attack seems to

work badly. The predicted drag in this paper is just used for qualitative trend analysis. The transient lift is larger than the steady result at high angles of attack, and the transient drag is larger than the steady one at all angles of attack, what's more, with the increase of  $t_{te}$ , the difference between the transient and steady drag increases dramatically. The reason for the difference between steady and transient results may be caused by the artificial restriction of flow to be two dimensional. In the future, Due to the special geometry of the blunt body of blunt trailing edge airfoils, three dimensional calculation and more accurate method such as DES even LES should be used to study the aerodynamic performance of blunt trailing edge airfoils.

With the increase of  $t_{te}$ , the increase rate and amount of lift becomes limited gradually at low angles of attack, while the drag increases dramatically. The larger  $t_{te}$  is, the higher the maximum lift is, but too large lift can cause abrupt stall. So the value of  $t_{te}$  should be constrained in a certain range. For example,  $t_{te}=5\%c$  is a better choice for blunt trailing edge airfoils, the lift of these airfoils has been increased but no abrupt stall.

The transient aerodynamic performances of blunt trailing edge airfoils are mainly influenced by the generation and shedding of blunt body vortices at low angles of attack and the combined effect of separation and blunt body vortices at large angles of attack. With the increase of  $t_{te}$ , the vibration amplitude of lift and drag curves increase, larger vibration amplitude of lift and drag may be harmful to the structure and power output of blade. Just as mentioned above, the value of  $t_{te}$  should be constrained in a certain range. There is a steady range of angles of attack for blunt trailing edge airfoils, in this range, the lift and drag curve vibrate more slightly than at other angles of attack, and the design angle of attack of blunt trailing edge airfoils should be set in this steady range.

Blunt trailing edge airfoils are mainly used in the inner part of the blades. For the inner part of the blades, the lift coefficient itself is very important, because in normal operating conditions, the local angle of attack can be very high. High values of  $C_{lmax}$  and good stall characteristics can help keep high aerodynamic performance. Blunt trailing edge airfoils can produce higher  $C_{lmax}$  and lift curve slope, but with the increase of  $t_{te}$ , the transient lift vibrates more violently and the stall characteristics deteriorates. So for the design of blunt trailing edge airfoils, from the aerodynamic point of view the characteristics of lift should be considered prior, the thickness of trailing edge should be constrained in a certain range to prevent the airfoil from abrupt stall and violent lift oscillation, the aerodynamic efficiency ( $C_l/C_d$ ) should also be considered but not so important as that for the tip part airfoils. From the structure point of view, the thickness of trailing edge should be as large as possible to increase the bending and distorting ability of airfoils, but this is conflicting with good aerodynamic performance. It's necessary to find a middle ground between aerodynamic and structure for the design of blunt trailing edge airfoils.

## 7. Acknowledgement

The study presented here is supported by the Energy Technology Development and Demonstration Program (EUDP project j.nr. 64011-0094) under the Danish Energy Agency, Funds of International Science and Technology Cooperation Program of China (No: 2010DFA64660), Research and Innovation Program for Graduates in Jiangsu Province (No: CXLX13-907), Open project of Hydraulic Engineering Laboratory of Jiangsu Province (No: K12019).

## References

- [1] Van Rooij R P J O M, Timmer W A. Roughness sensitivity considerations for thick rotor blade airfoils. *Journal of Solar Energy Engineering* 2003, **125**(4): 468-478.
- [2] Jackson K J, Zuteck M D, et al. Innovative design approaches for large wind turbine blades. *Wind Energy* 2005; **8**: 141-171.
- [3] Standish K J, van Dam C P. Aerodynamic analysis of blunt trailing edge airfoils. *Journal of Solar Energy Engineering* 2003; **125**: 479-487.
- [4] Matthew F B, Dale B. Aerodynamic and aeroacoustic properties of a flatback airfoil: an update. *Proc. of the 47<sup>th</sup> AIAA Aerospace Sciences Meeting*, 2009.

- [5] Baker J P, van Dam C P, Gilbert B L. Flat back airfoil wind tunnel experiment, Sandia National Laboratories, California, USA. 2008. SAND2008-2008.
- [6] Baker J P, Mayda E A, van Dam C P. Experimental analysis of thick blunt trailing-edge wind turbine airfoils. *Journal of Solar Energy Engineering*, 2006; **128**: 422-431.
- [7] Law S P, Gregorek G M. Wind tunnel evaluation of a truncated NACA 64-621 airfoil for wind turbine applications. NACA CR-180803, 1987.
- [8] van Dam C P, Mayda E A, Chao D D, et al. Computational design and analysis of flatback airfoil wind tunnel experiment, Sandia National Laboratories, California, USA. 2008. 2008-1782.
- [9] Matthew F B. Numerical simulation of flatback airfoil for wind turbine applications. University of Louisville, 2009.
- [10] Chao D D, van Dam C P. Computational aerodynamic analysis of a blunt trailing-edge airfoil modification to the NREL phase VI rotor. *Wind Energy*, 2007; **10**: 529-550.
- [11] Timmer W A, van Tooiij RPJOM. Summary of the Delft University wind turbine dedicated airfoils. *Journal of Solar Energy Engineering*, 2003; **125**: 488-496.
- [12] Drela M. XFOIL: An analysis and design system for low Reynolds number airfoils. *Lecture Notes in Engineering*, 1989; **54**: 1-12.
- [13] Deng Lei, Qiao Zhide, Yang Xudong, et al. Aerodynamic performance computational of trailing-edge-blunting methods of flat back airfoil for large wind turbine based on RANS equation. *Acta Energetica Solaris Sinica*, 2012; **33**(4): 545-551.
- [14] Menter F R. Two-Equation Eddy-Viscosity Turbulence Models for Engineering Applications. *AIAA Journal*, 1994; **32**(8): 1598-1605.
- [15] Menter F R, Langtry R B, Likki S R, et al. A correlation-based transition model using local variables, part I -model formulation. *In proceedings of ASME Turbo Expo 2004, Power for Land, Sea, and Air*, Vienna, Austria, 14-17 June 2004. ASME. GT2004-53452.
- [16] Menter F R, Langtry R B, Likki S R, et al. A correlation-based transition model using local variables, part II –test cases and industrial applications. *In proceedings of ASME Turbo Expo 2004, Power for Land, Sea, and Air*, Vienna, Austria, 14-17 June 2004. ASME. GT2004-53454.
- [17] ROHA. LSWT report on selected DU profiles. LM WIND Power, 2012.
- [18] Shelton A, Abras J, Jurenko R et al. Improving the CFD predictions of airfoils in stall. *43<sup>rd</sup> AIAA Aerospace Sciences Meeting and Exhibit*, Reno, Jan, 2005. AIAA Paper No. AIAA-2005-1227.
- [19] Drela M, Giles M B. Viscous-inviscid analysis of transonic and low Reynolds number airfoils. *AIAA Journal*, 1987; **25**(10): 1347-1355.